Materials Characterization 160 (2020) 110132

Contents lists available at ScienceDirect

Materials Characterization

journal homepage: www.elsevier.com/locate/matchar

A comparison of the dry sliding wear behavior of NiCoCr medium entropy alloy with 316 stainless steel

Xiaobin Guo[a,b], Ian Baker[a,*], Francis E. Kennedy[a], Min Song[c]

[a] Thayer School of Engineering, 14 Engineering Drive, Dartmouth College, Hanover, NH 03755-8000, USA
[b] School of Materials Science and Engineering, Central South University, Changsha 410083, China
[c] State Key Laboratory of Powder Metallurgy, Central South University, Changsha 410083, China

ARTICLE INFO

Keywords:
Medium entropy alloys
Wear properties
Scanning electron microscopy
X-ray photoelectron spectroscopy

ABSTRACT

The aim of this work was to determine the wear behavior of the f.c.c. medium entropy alloy NiCoCr, which has been shown by others to possess both a very good strength-ductility balance and an especially high fracture toughness. Pins of NiCoCr were tested in dry sliding wear against disks of yttria-stabilized zirconia at a sliding velocity of 0.1 m/s both in air and in argon. Identical wear tests on 316 stainless steel were performed for comparison. It was found that the wear rates of the NiCoCr pins were lower than those of the 316 stainless steel in air, but that the wear rates of the two materials were almost identical in dry argon. Scanning electron microscopy analysis of both the worn pins' surfaces and cross sections indicated that the worn surface of NiCoCr pins were flatter and showed less fracture due to the better toughness compared to the 316 stainless steel pins. Wear tests in air resulted in the formation of oxides. X-ray photoelectron spectroscopy of the NiCoCr pin showed that the oxides in the debris were Cr_2O_3 and Co_2O_3. The oxides play an important role in the development of a mechanically mixed layer, which formed on the NiCoCr pin's tip to protect the contacting material during wear tests in air.

1. Introduction

The equi-atomic NiCoCr medium entropy alloy exhibits an extremely high room temperature fracture toughness above 200 MPa $m^{1/2}$, as demonstrated by Gludovatz et al. [1]. The alloy, which is a single-phase f.c.c. solid solution, shows even better strength and ductility with decreasing temperature. Indeed, the alloy shows a good balance of strength and ductility over the temperature range from −196 °C to 400 °C [1–3], while the results of fracture toughness tests showed that the NiCoCr medium-entropy alloy represents one of the toughest materials in any materials class ever reported [1].

There have been several studies of the room temperature wear behavior of both bulk high entropy alloys (HEAs) and HEA coatings [4–7], which have generally been of the sliding pin-on-disk type conducted at room temperature in air. Tsai and Yeh [8] discussed the wear properties of HEAs and noted that the wear resistance of f.c.c. single-phase HEAs increased with increasing hardness, a well-known feature referred to as the Archard law [9,10], i.e.

$$W = K F L/H \quad (1)$$

where W is the volume loss of materials through wear, K is the wear coefficient, F is the normal load, L is the sliding distance, and H is the hardness of the material. Tsai and Yeh [8] found that HEAs containing an ordered second phase had improved wear resistance, especially if the second phase was hard and was the majority phase. Thus, compared to the wear behavior of 52100 (SUJ2) bearing steel, the wear resistance of the HEA $Al_{0.2}Co_{1.5}CrFeNi_{1.5}Ti$ is 3.6 times better, even though these two materials have similar hardness values [4]. Similarly, the HEA $Co_{1.5}CrFeNi_{1.5}Ti$ has a wear resistance comparable to that of H13 tool steel even though the hardness of H13 steel is greater [4]. Very recent wear testing of NiCoCr against an Inconel 718 counterpart at elevated temperatures found much lower wear rates at higher sliding temperatures, and concluded that the wear mode changes from abrasive wear at room temperature to oxidative and adhesive wear at 200 °C. However, the authors of [11] didn't investigate the important effect of environment on the wear rate of the materials and didn't consider the contribution of frictional heating to the contact temperature during sliding wear tests.

Sliding contact produces substantial heating during the wear tests as energy is transformed from the friction force, which results in a temperature increase of the contact area of the pins [12]. The temperature increase can influence the pin's hardness and make plastic deformation

* Corresponding author.
E-mail address: Ian.Baker@Dartmouth.edu (I. Baker).

https://doi.org/10.1016/j.matchar.2020.110132
Received 14 September 2019; Received in revised form 3 January 2020; Accepted 10 January 2020
Available online 11 January 2020

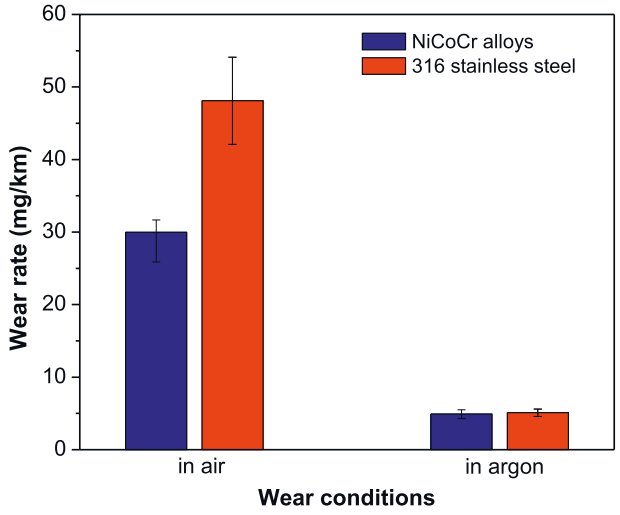

Fig. 1. Wear rates of NiCoCr alloys and 316 stainless steel pins in air and argon atmosphere against YSZ disk. The results are the average of three tests, and error bars from range of data.

in the pin/disk contact area much easier. The wear rate also changes with hardness according to Eq. (1). This temperature increase can also lead to greater oxidation of the pin tip. In iron-based metals, it is thought that an oxide film forms on the surface that could increase the wear resistance [13]. Although an oxide could work as protection of the metallic surface during wear, it may break off to produce wear particles, i.e. wear debris [14]. When wear tests are performed at a slow speed and limited load with the contact temperature lower than 400 °C, the oxides in iron-based alloys are usually soft and part of the oxide film spalls to produce mild oxidative wear [14]. If the wear debris is much harder than the metal layer, it could lead to severe wear, which has been found in NiAl-based alloys [15].

This work is a study of the wear behavior of equi-atomic NiCoCr using pin-on-disk sliding wear tests against an yttria-stabilized zirconia (YSZ) disk in both air and argon. These results are compared with those from similar tests performed on 316 stainless steel, which is a single-phase austenitic alloy that exhibits good oxidation and corrosion resistance at relatively low cost and is used in numerous applications, despite its suboptimal wear resistance. It is of interest to study if the higher yield strength of NiCoCr compared to 316 stainless steel will produce better wear resistance.

2. Materials and methods

An ingot of equi-atomic NiCoCr alloy was prepared by arc-melting elemental Ni, Co and Cr (purities > 99.9%) under argon. The ingot was melted three times and flipped to another face before the next melting to ensure homogeneity. The alloy was then placed in a Bridgeman furnace and a rod 71 mm long and 12 mm diameter was produced. Both the NiCoCr rod and a commercial 10 mm diameter 316 stainless steel rod were machined into pins 19 mm long, 9.5 mm diameter with hemispherical tips. All pins were polished to a mirror finish. The counterface was a 10 cm diameter disk of YSZ containing 2.8 mol% yttria produced by Saint-Gobain Advanced Ceramics. The hardness of NiCoCr and 316 stainless steel were measured by TH713 Vickers hardness tester with 2.94 N load and 15 s loading time. The YSZ disk was polished to a surface roughness of < 0.05 μm, and had a measured Vickers hardness of 1339 ± 50 HV.

In order to evaluate the influence of oxygen, pin-on-disk wear tests were performed in both air and argon using a previously-described system [15]. The normal load on the pins was 23 N and the sliding distance was 1 km for each test. All the tests were performed at 0.1 m/s sliding velocity at room temperature (approximately 25 °C) and each test was run on an unworn portion of the YSZ disk surface. Wear debris were collected from the disk after wear test using adhesive tape. Wear tests for each condition and for both alloys were repeated three times.

In order to study the effect of third bodies on the wear behavior of NiCoCr, a brush was used to remove the wear debris during the wear tests in air. The brush was wide enough to remove the debris from the wear tracks on the YSZ disk.

The mass losses of the pins were calculated by measuring the mass of wear pins before and after test using a balance of ± 0.1 mg precision.

The worn surface and cross section of NiCoCr alloy and 316 stainless steel pins were analyzed using a FEI Scios2 LoVac dual beam scanning electron microscope (SEM) operated at 30 kV equipped with EDAX SDD X-ray detector (EDS). The cross sections of pins were prepared by cutting pins through the center of the worn area using a diamond saw; then the cross sections were mechanically polished.

X-ray photoelectron spectroscopy (XPS) measurements were obtained from the worn surface of NiCoCr using a spectrometer (ESCALAB

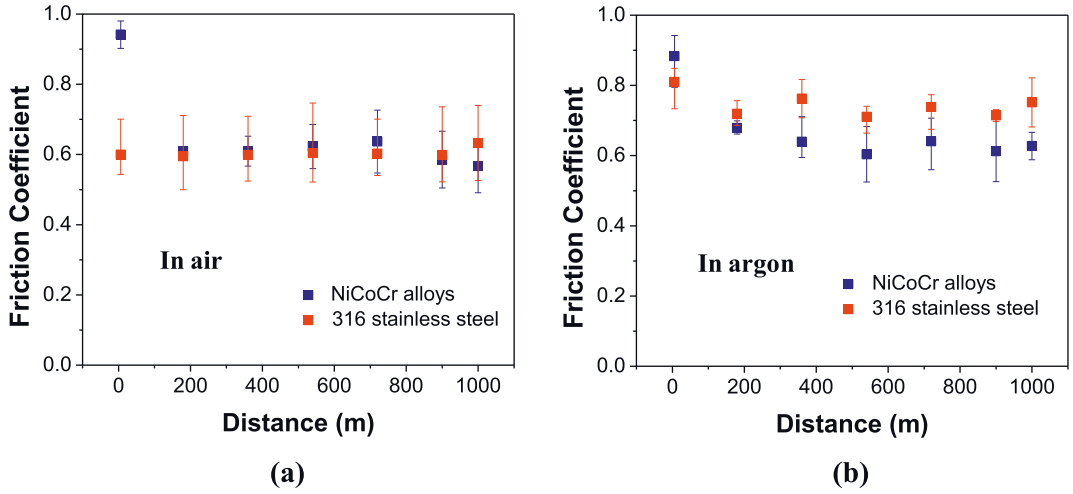

Fig. 2. Friction coefficient of NiCoCr and 316 stainless steel pins under different atmospheres against YSZ disk: (a) in air; (b) in argon.

250; Thermo Fisher Scientific) in order to determine the specific oxide present.

After wear tests in air or argon, the surfaces of the worn pins were characterized using a Phase Shift micron XAM surface mapping microscope, through which the depths of wear grooves of pins were measured.

3. Results

3.1. The wear behavior of NiCoCr alloys and 316 stainless steel pins

The results from wear tests of NiCoCr alloys and 316 stainless steel pins performed against YSZ disks at room temperature in air and argon are shown in Fig. 1. Three tests were conducted to obtain the average wear rates of each alloy under the different atmospheres and to calculate the error bars. The two materials both have much greater mass loss after wear tests in air compared to tests under argon. The NiCoCr pins had an average mass loss of 31 mg in air and 4.9 mg in argon, while the 316 stainless steel pins had a mass loss of 48 mg in air and 5.1 mg in argon. It is clear that NiCoCr has greater wear resistance than 316 stainless steel in air, but shows similar behavior under argon. The Vickers hardness of the 316 stainless steel pins and NiCoCr pins are 152 HV and 185 HV, respectively. According to the Archard equation, the wear rate decreases with the increase of hardness and yield strength of the material, thus the NiCoCr alloys would be expected to show a lower wear rate.

Fig. 2(a) shows friction data for the two alloys tested in air, while Fig. 2(b) shows values for tests under argon. At the very beginning of the tests the friction coefficient had its highest value of ~0.9 for NiCoCr alloy pins in both air and argon, while the initial friction coefficient of 316 stainless steel was 0.6–0.8. With increasing sliding distance, the friction coefficient dropped to a steady-state value near 0.6 for both NiCoCr and 316 stainless steel in air. The reason for the drop in friction is that an oxide film and the mechanically mixed layer that formed on the contacting area led to a decrease in friction. Under argon, the value for the 316 stainless steel steady state friction coefficient was 0.7–0.8, which is higher than the 0.6–0.65 for the NiCoCr alloy.

The surfaces of the worn pins of NiCoCr and 316 stainless steel were characterized using a SEM/EDS. The surfaces of the worn pins after wear tests in air were relatively smooth and flat, as shown in Fig. 3(a) and (b), especially those of the NiCoCr alloys (Fig. 3(a)). The surfaces of pins worn under argon atmosphere revealed mild abrasion, as shown by the worn grooves in Fig. 3(c) and (d). EDS results from the worn surface shown in Fig. 3 are shown in Fig. 4. Comparing the results from the NiCoCr alloy wear test in air to the EDS of worn surface tested under argon (compare Fig. 4(a) and (c)), there are only minor differences in the X-ray peaks from the metallic elements, but the relative oxygen amount, which comes from comparing the oxygen peak with the metal peak, is significantly lower for the tests in argon. This is reasonable as fewer oxides were produced with the limited amount of oxygen available during wear test under argon. The results from 316 stainless steel are almost the same, except a small peak from zirconium appeared on the worn surface after the wear test under argon (Fig. 4(d)). Notice that there is no zirconium peak from the NiCoCr pins' worn surface.

The wear grooves on the worn pin surfaces were characterized using a micro XAM profilometer, and the 3D reconstructed images are shown in Fig. 5. The worn surface of NiCoCr pin after wear testing in air was flat and relatively smooth, see Fig. 5(a). In contrast, the 316 stainless

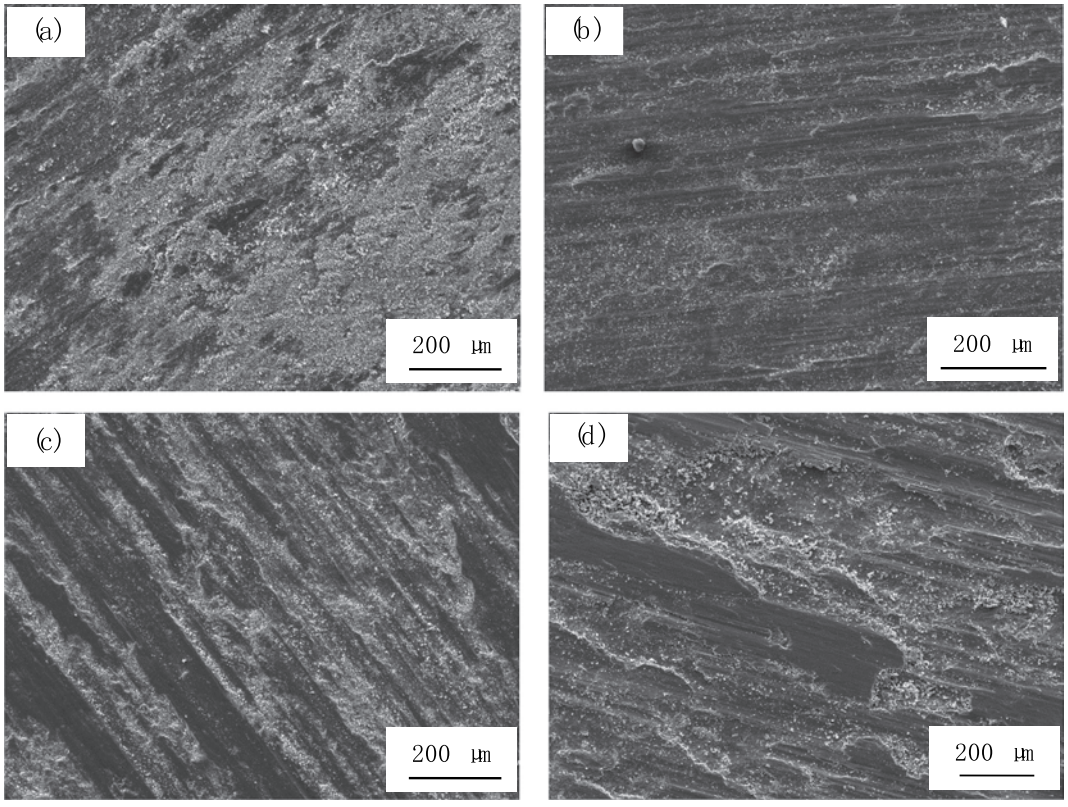

Fig. 3. Secondary electron images of pin surfaces of the two materials after wear tests against YSZ disk at 0.1 m/s under different atmospheres: (a) NiCoCr in air; (b) 316 stainless steel in air; (c) NiCoCr under argon; (d) 316 stainless steel under argon.

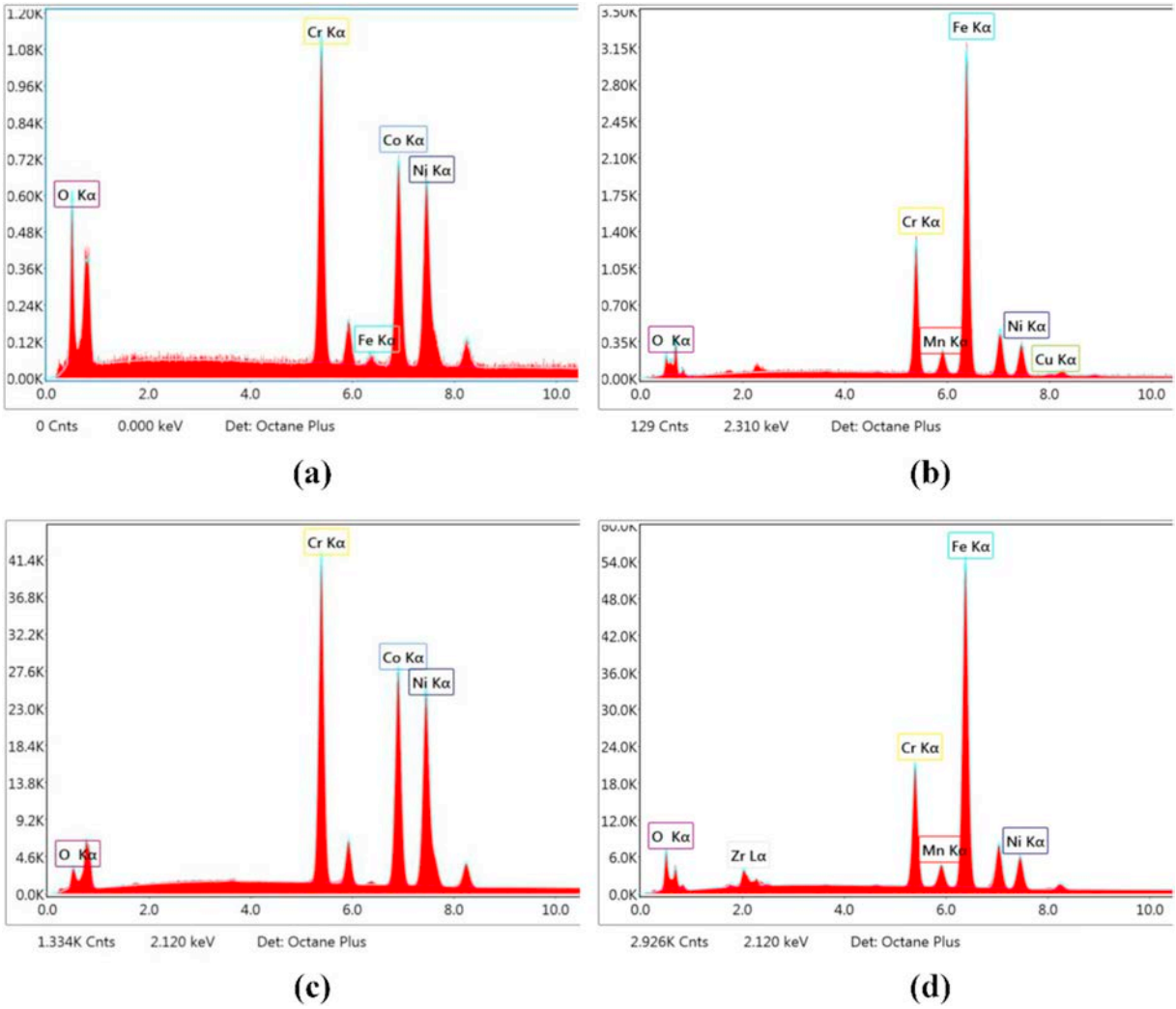

Fig. 4. EDS point spectra from pin surfaces after wear tests against YSZ disk at 0.1 m/s under different atmospheres: (a) NiCoCr in air; (b) 316 stainless steel in air; (c) NiCoCr under argon; (d) 316 stainless steel under argon.

steel showed a much rougher worn surface after wear in air; as is seen in Fig. 5(b), three grooves were formed with almost the same depth and width. The surfaces after wear under argon showed the presence of grooves for both the NiCoCr pin (Fig. 5(c)) and the 316 stainless steel pin (Fig. 5(d)), for which the grooves were wider. The depths of the grooves were measured and are listed in Table 1. The results indicated that the NiCoCr pin has a less worn surface compared to the 316 stainless steel in both air and argon, and the NiCoCr pin had shallower grooves after wear tests in argon. It should be noted that the presence of grooves such as those shown in Fig. 5(b–d) is indicative of more abrasion of the pin surfaces in those cases.

3.2. Influence of wear particles on wear of NiCoCr against YSZ

The wear debris collected from the YSZ disks after the wear tests were also examined using a SEM/EDS. As shown in Fig. 6(a) and (c), the debris from the NiCoCr tests in air had a diameter of up to ~50 μm, while the debris particles from wear under argon were < 20 μm in diameter. There was little difference in the EDS spectra from the two samples, see Fig. 6(b) and (d). The results from 316 stainless steel pins were different. After wear tests in air, the debris diameter was about 25 μm (Fig. 6(e)), while large particles with near 100 μm size were produced from wear tests under argon (Fig. 6(g)). The EDS spectra from the two kinds of debris also showed little difference. It is interesting to note that minor peaks of zirconium appeared in Fig. 6(d), (f) and (h), but not in the debris from NiCoCr pins after wear testing in air (Fig. 6(b)).

The volumetric wear rate of YSZ disks has been measured after each wear test, and the results are shown in Fig. 7. Wear of the NiCoCr pin led to greater volume loss of the counterface YSZ disk during wear tests in air than in argon. This indicated that hard third bodies, probably oxide particles, may have abraded the disk within the contacting area during tests in air. The primary difference between the two wear atmospheres is the oxygen concentration, thus oxide formation is the main influence factor. It was also found that the NiCoCr pin led to more volume loss of the disk than did the 316 stainless steel pin in the air

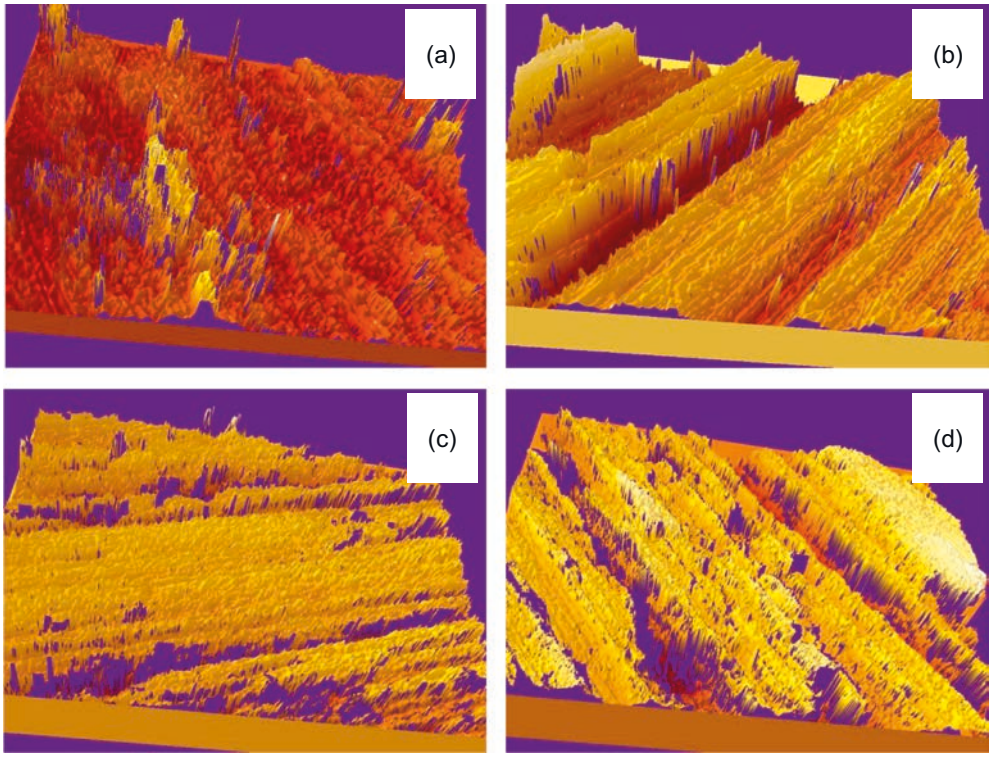

Fig. 5. Wear grooves on the pins (a) NiCoCr in air; (b) 316 stainless steel in air; (c) NiCoCr in argon; (d) 316 stainless steel in argon.

Table 1
Depth of wear grooves of NiCoCr and 316 stainless steel pins after wear test in air or argon at 0.1 m/s with a normal load of 23 N for a sliding distance of 1 km.

Atmosphere	Depth of grooves (μm) NiCoCr	Depth of grooves (μm) 316 stainless steel
Air	3.03	5.11
Argon	7.83	14.3

condition, whereas the NiCoCr pin suffered less wear than did the 316 stainless steel pins in air. This indicated that oxides protect NiCoCr alloys better than 316 stainless steel.

In order to determine which types of oxide are found on NiCoCr pin surfaces after being wear tested in air, XPS was performed on the worn surface. The results for the three elements Co, Cr and Ni are shown in Fig. 8. The Co 2p spectrum from the worn surface indicated that a single constituent of Co_2O_3 (781.1 eV of $2p_{3/2}$, 786.3 eV of $2p_{3/2,\ sat}$, 797.2 eV of $2p_{1/2}$ and 803.9 eV of $2p_{1/2,\ sat}$) was produced, while the Cr 2p spectrum indicated a single constituent of Cr_2O_3 (576.8 eV of $2p_{3/2}$, 586.7 eV of $2p_{1/2}$) was produced. Comparison with the reference oxide peaks for Co, Cr and Ni marked shows that the main oxides present were Co_2O_3 and Cr_2O_3 [16].

An SEM was also used to characterize the microstructures of the cross-sections of worn pins, as shown in Fig. 9, and the mechanically mixed layer is marked by yellow lines. The microstructures were different for NiCoCr and 316 stainless steel after wear tests in air, such as Fig. 9(a) and (b); the depth of mechanically mixed layer on the NiCoCr pin's tip was approximately 12 μm, while no obvious mechanically mixed layers were found on the worn 316 stainless steel pins. The depth of mechanical-mixed layer on tips of NiCoCr and 316 stainless steel pins after wear tests in argon were the same at about 8 μm, as shown in Fig. 9(c) and (d). EDS point spectra were obtained at the locations noted as Spot 1 on Fig. 9(a–d), and the results are shown in Fig. 10. The EDS results of NiCoCr and 316 stainless steel pins after wear tests in air (Fig. 10(a) and (b)) indicated that more oxides (more oxygen) appeared in the mechanical mixed layer on NiCoCr pin's tip than for 316 stainless steel.

In order to understand the influence of oxides on wear behavior, a brush was used to sweep away the wear debris from the YSZ disk during wear tests. The stationary brush was placed at a point on the YSZ disk surface just after the surface exited from the pin contact. The wear rates of NiCoCr and 316 stainless steel pins during wear tests with brush present are shown in Fig. 11. The NiCoCr pin has more mass loss after wear testing with a brush present compared to the without-brush-condition, while the 316 stainless steel pin has less mass loss. The results indicate that removal of third bodies such as oxide particles can have a negative effect on the wear resistance of NiCoCr pins during wear tests. This may be attributed to fewer hard oxide particles in the protective mechanically mixed layer on the worn surface as the wear debris has been swept away. On the other hand, hard third-body wear particles may have contributed to wear of pin surfaces, so removing those particles with a brush could have resulted in lower wear, as was seen for the 316 stainless steel pins. The friction coefficients of the pins worn with a brush present are shown in Fig. 12. Both NiCoCr and 316 stainless steel pins have slightly higher friction coefficients with a brush present during the wear tests against YSZ than without brush condition, so the wear debris may have contributed to a small reduction in friction.

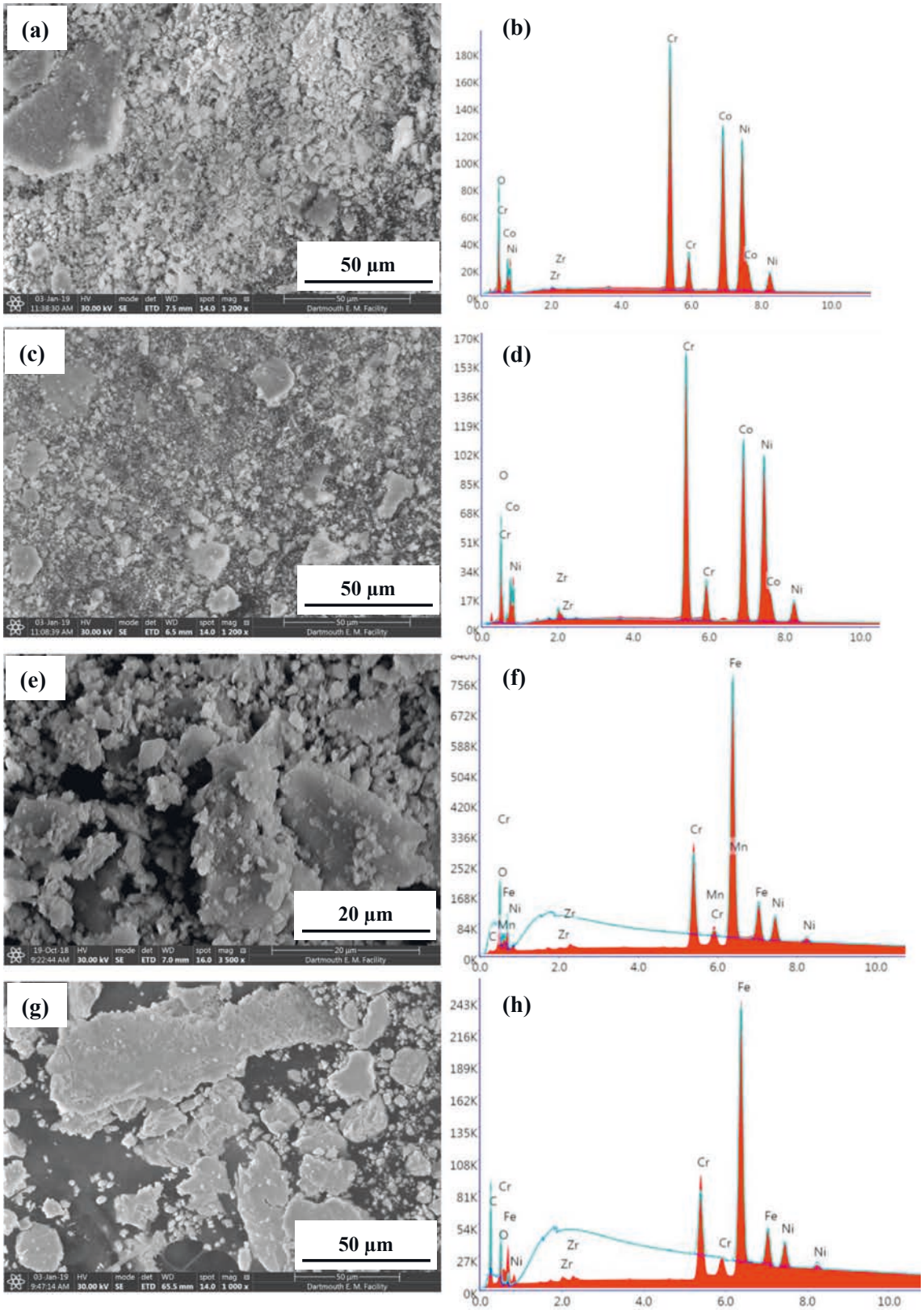

Fig. 6. Secondary images and EDS point spectra from wear debris collected during wear tests against YSZ disk at 0.1 m/s under different atmospheres: (a) and (b) NiCoCr in air; (c) and (d) NiCoCr under argon; (e) and (f) 316 stainless steel in air; (and g) and (h) 316 stainless steel under argon.

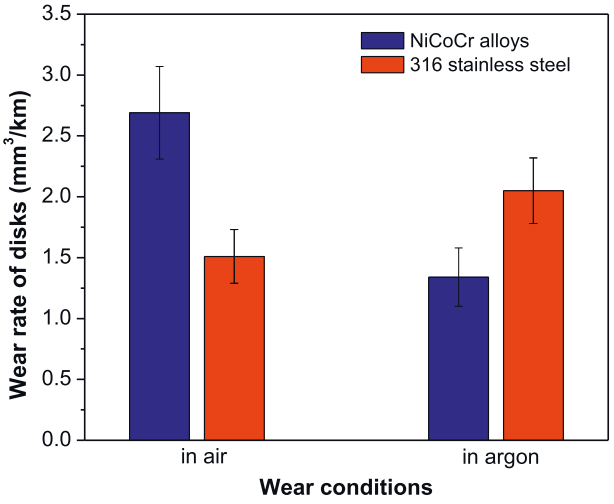

Fig. 7. The volumetric wear rates of YSZ disks for tests conducted in two different atmospheres.

4. Discussion

The results in Fig. 1 indicated that the mass loss of the NiCoCr pins during wear tests against YSZ was less than that for 316 stainless steel pins, especially in air. This may be partially attributed to the higher hardness of the NiCoCr material, as predicted by the Archard law. The material's toughness can also influence its wear performance, particularly through its influence on abrasion. The failure strain of NiCoCr alloys during tensile tests at room temperature is 70% [1], while this value is 40% for 316 stainless steel [17]. As shown in Fig. 3, the worn surface of NiCoCr pins had fewer fracture features. The wear grooves in Fig. 5 also indicated that the worn surface of NiCoCr pins has shallower grooves due to the better toughness and better abrasion resistance.

The results of this work can be compared with those of the recently published study of wear of a similar CoCrNi medium entropy alloy [11], since both studies included tests run at 0.1 m/s sliding speed in room temperature air. It was found that the steady-state friction coefficients for the two studies were remarkably similar (0.6–0.65) for tests done in similar conditions, even though the counterface materials were different (YSZ in this case and Inconel 718 for the Pan, et al. study [11]). The worn surfaces of the CoCrNi pins in both studies showed considerable plastic deformation, although the deformed and mechanically mixed surface layers in this study were found to contain oxides (Figs. 9a and 10a), whereas no oxides were noted on the worn surfaces of [11]. The oxides likely imparted some wear resistance to the surfaces in this study. As a result, wear rates from [11] were nearly seven times greater than those measured here for similar test conditions, after accounting for the different normal loads in the two cases (5 N in [11], but 23 N here). The greater normal force and lower thermal conductivity of the YSZ disk in this work resulted in higher contact temperatures, causing more oxidation at 0.1 m/s sliding speed than was noted in tests done on an Inconel 718 disk [11].

Because the contact temperature between the pin and disk is increased by frictional heating during the wear tests, the contacting surface could react with the oxygen to produce oxides on the surface [12–14]. The thermal conductivity of NiCoCr alloys is 15 W/(m*K) [18], while that for 316 SS is 12.9 W/(m*K) [19]. The maximum contact temperature at 0.1 m/s sliding speed was calculated, using the methods of reference [12], to be approximately 180 °C for the NiCoCr pins and 166 °C for the 316 stainless steel pins. The low contact temperatures indicate that temperature effects on the wear behavior of these two materials are negligible. The alloy's composition would be the

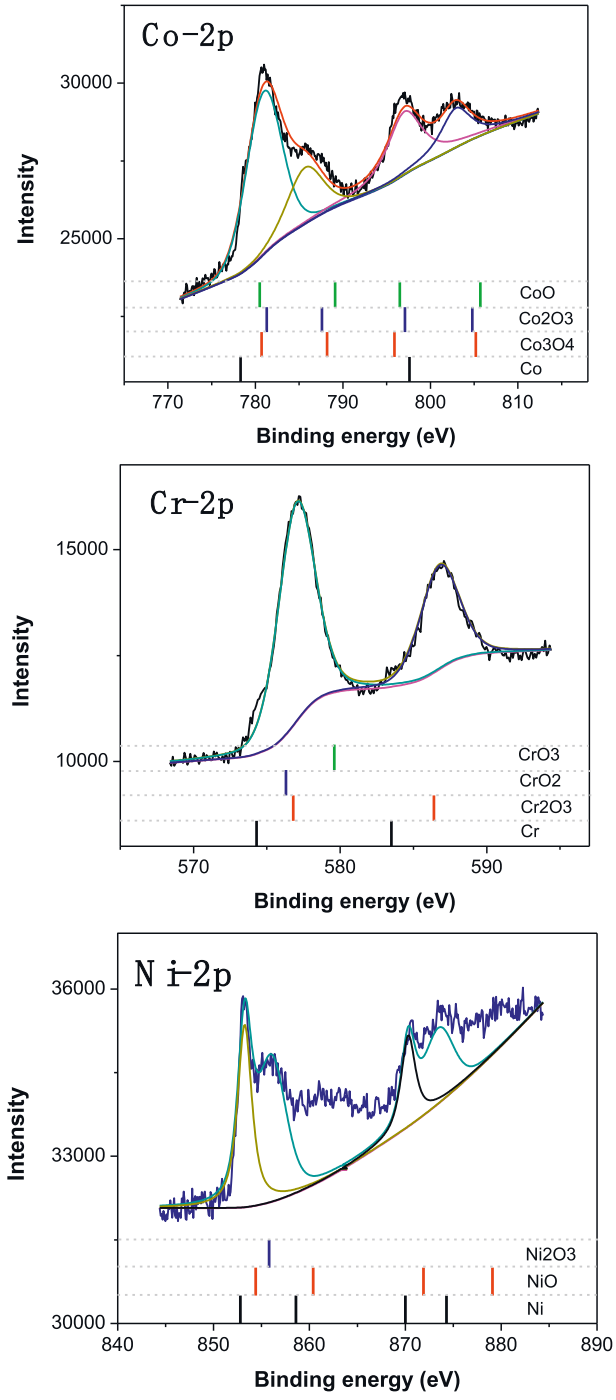

Fig. 8. X-ray photoelectron spectroscopy from the worn surface of NiCoCr pin after wear test at 0.1 m/s against YSZ in air.

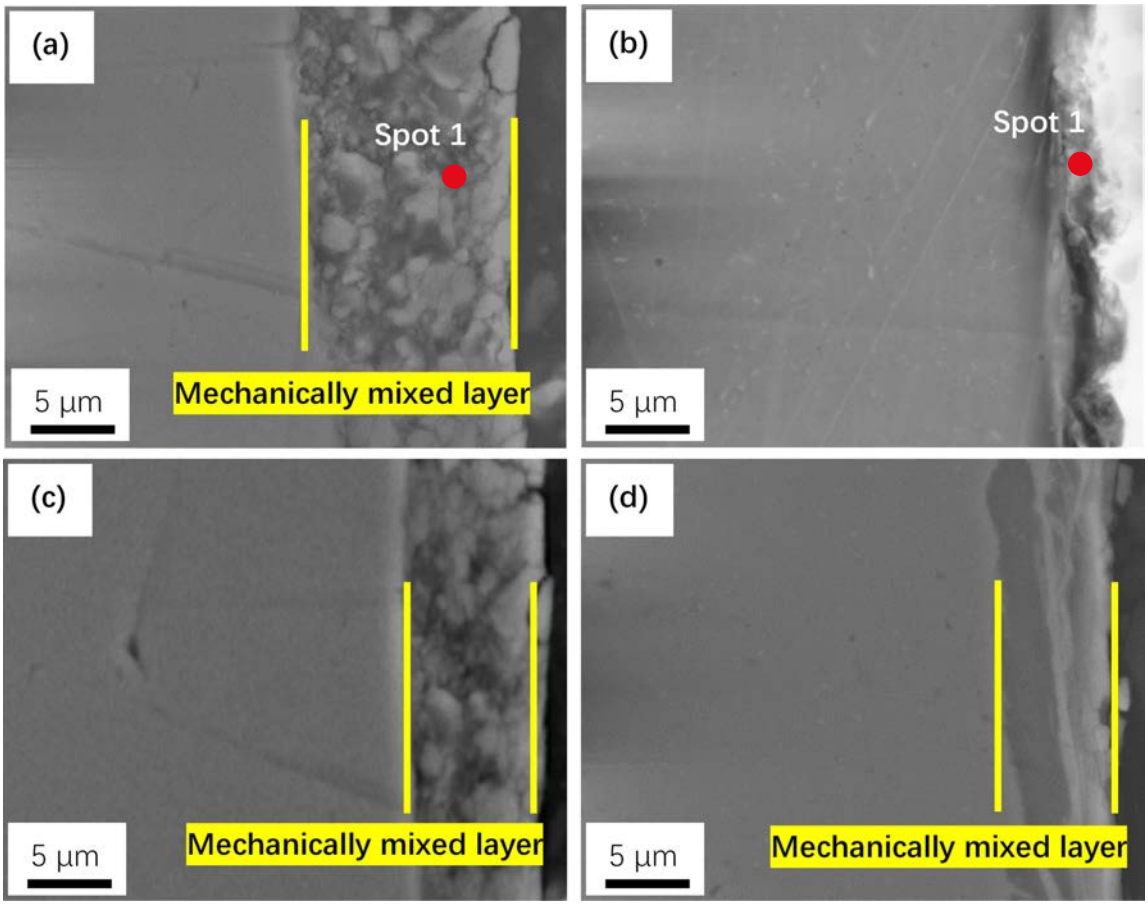

Fig. 9. Secondary electron images of the cross-sections of worn pins after wear tests again YSZ disk at 0.1 m/s (a) NiCoCr in air; (b) 316 stainless steel in air; (c) NiCoCr under argon; (d) 316 stainless steel under argon.

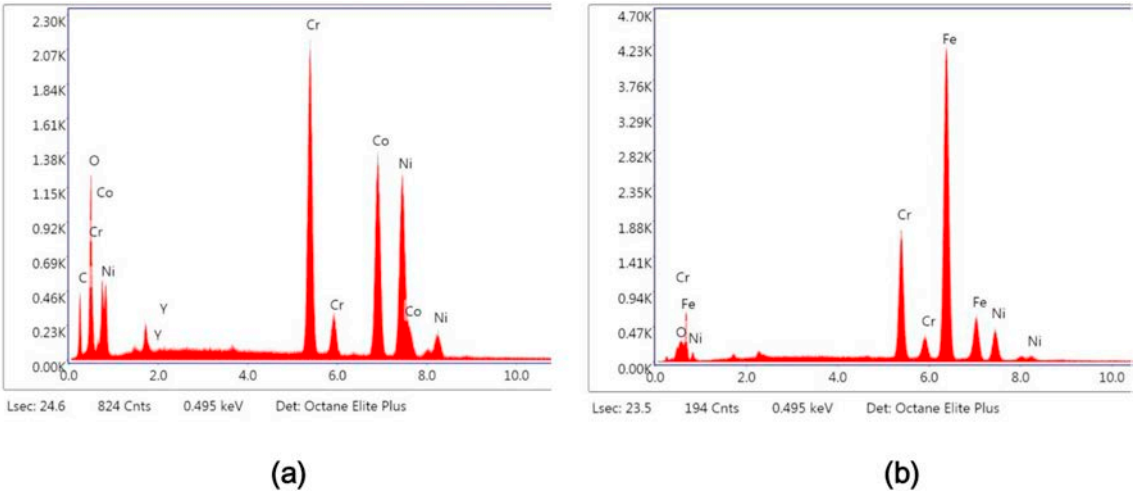

(a) (b)

Fig. 10. EDS point spectra of the cross-sections of worn pins after wear tests against YSZ disk at 0.1 m/s (a) NiCoCr in air; (b) 316 stainless steel in air.

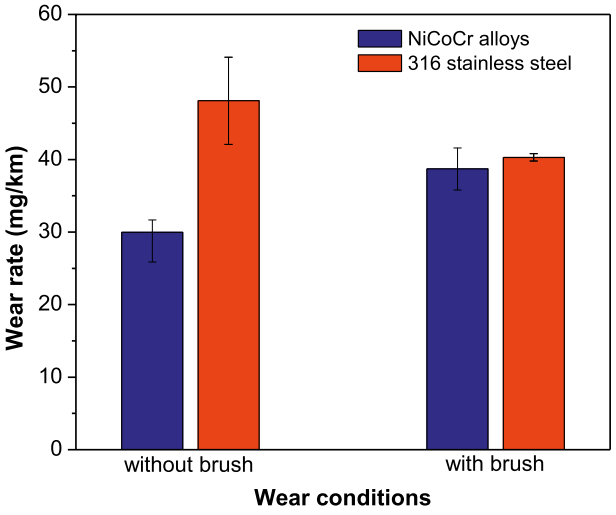

Fig. 11. Wear rates of NiCoCr alloys and 316 stainless steel pins in air against YSZ disk with or without brush present. The results are the average of three tests.

main influence factor. As the EDS results show in Fig. 4(a) and (b), the oxygen peaks were intense after the wear tests in air for both worn NiCoCr and 316 stainless steel pin surfaces. The results of wear tests in argon, as indicated in Fig. 4(c) and (d), barely showed any oxygen peaks. The oxide layer formed at the contact area of the pin and disk can protect the contacting material of the pins during wear tests, particularly when the oxide is incorporated in the mechanically mixed layer. This was demonstrated when the mass loss of the NiCoCr pin increased in tests with a brush present (Fig. 11). EDS analysis of collected wear debris in Fig. 5 indicated that the debris from the wear tests in air had large oxygen peaks, which means that the debris contained oxides formed during sliding. Much of the debris must have been harder than the surface and abraded the surface, resulting in wear rates in air that were significantly higher than those in argon.

The results of wear rates with the brush present (Fig. 11) indicate that removing the wear debris increases the wear rate for the NiCoCr pin, suggesting that the oxides on the pin's surface can play an important role in the production of the protective mechanically mixed layer. This hard mechanically mixed layer on the worn surface incorporates the oxides and other components from the wear debris during the shear deformation process of wear testing, and the layer then reduces the rate of further wear of that surface [20]. The microstructures of the pin's tip (Fig. 9) also indicated that NiCoCr alloys has deeper mechanically mixed layer, resulting in wear resistance that is higher (lower wear rate) than that of 316 stainless steel.

5. Summary

Dry sliding pin-on-disk wear tests of NiCoCr alloy against yttria-stabilized zirconia were conducted in air and argon and the results compared to tests on 316 stainless steel. The results and comparison indicate that:

1. The wear rate of the NiCoCr pins in air at 0.1 m/s velocity was much lower than the wear rate of the 316 stainless steel: the wear rates of the NiCoCr and the 316 stainless steel under argon were similar and much lower than the wear rates in air.

2. The worn surfaces of NiCoCr pins were smoother and showed less fracture and abrasion due to the higher toughness compared to the 316 stainless steel pins. The NiCoCr pin's tip produced a deeper mechanically mixed layer than 316 stainless steel after wear testing in air.

3. Oxidation of the NiCoCr pins results in the formation of hard oxides during wear tests in air, while fewer oxides were present in the debris from wear tests under argon. The oxides found in the wear debris formed during the wear tests were Cr_2O_3 and Co_2O_3 for the NiCoCr pins.

4. The oxides became embedded in a hard mechanically mixed layer that formed on the NiCoCr pin's tip and protected the contacting material of the pins during wear tests in air.

Declaration of competing interest

There is no conflict of interest.

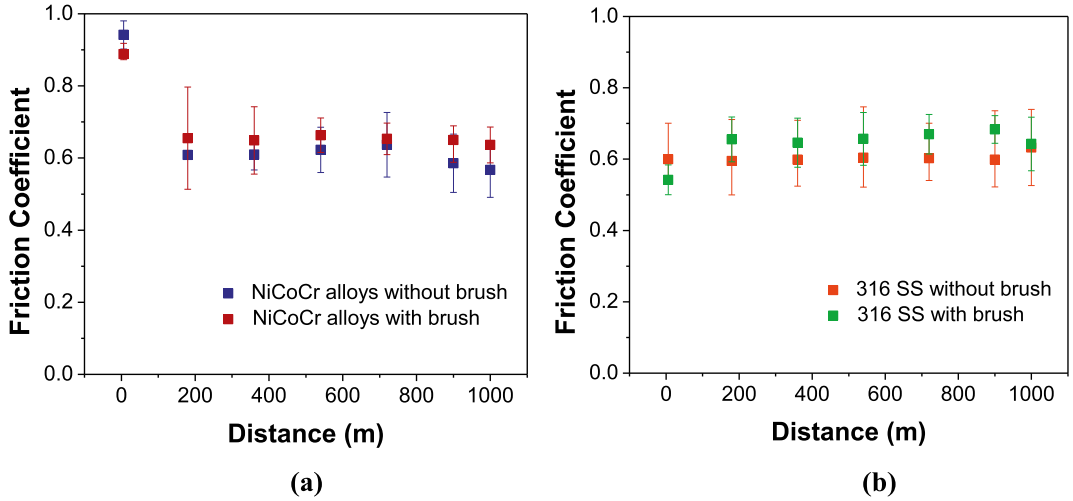

Fig. 12. Friction coefficients of pins wear against YSZ disk with or without brush: (a) NiCoCr; (b) 316 stainless steel.

Acknowledgements

This work was supported by National Science Foundation grant number 1758924.

References

[1] B. Gludovatz, A. Hohenwarter, K.V.S. Thurston, H. Bei, Z. Wu, E.P. George, R.O. Ritchie, Exceptional damage-tolerance of a medium-entropy alloy CoCrNi at cryogenic temperatures, Nat. Commun. 7 (10602) (2016) 1–8.
[2] Z. Wu, H. Bei, F. Otto, G.M. Pharr, E.P. George, Recovery, recrystallization, grain growth and phase stability of a family of FCC-structured multi-component equiatomic solid solution alloys, Intermetallics 46 (2014) 131–140.
[3] Z. Wu, H. Bei, G.M. Pharr, E.P. George, Temperature dependence of the mechanical properties of equiatomic solid solution alloys with face-centered cubic crystal structures, Acta Mater. 81 (2014) 428–441.
[4] M.H. Chuang, M.H. Tsai, W.R. Wang, S.J. Lin, J.W. Yeh, Microstructure and wear behavior of $Al_xCo_{1.5}CrFeNi_{1.5}Ti_y$ high-entropy alloys, Acta Mater. 59 (2011) 6308–6317.
[5] J.B. Cheng, X.B. Liang, B.S. Xu, Effect of Nb addition on the structure and mechanical behaviors of CoCrCuFeNi high-entropy alloy coatings, Surf. Coat. Technol. 240 (2014) 184–190.
[6] L. Jiang, W. Wu, Z. Cao, D. Deng, T. Li, Microstructure evolution and wear behavior of the laser cladded $CoFeNi_2V_{0.5}Nb_{0.75}$ and $CoFeNi_2V_{0.5}Nb$ high-entropy alloy coatings, J. Therm. Spray Technol. 25 (2016) 806–814.
[7] A. Poulia, E. Georgatis, A. Lekatou, A.E. Karantzalis, Microstructure and wear behavior of a refractory high entropy alloy, Int. J. Refract. Met. Hard Mater. 57 (2016) 50–63.
[8] M.H. Tsai, J.W. Yeh, High-entropy alloys: a critical review, Materials Research Letters 2 (2014) 107–123.
[9] J.F. Archard, Contact and rubbing of flat surfaces, J. Appl. Phys. 24 (1953) 981–988.
[10] J.F. Archard, W. Hirst, Wear of metals under unlubricated conditions, Proc. of the Royal Society of London. Series A, Mathematical and Physical Sciences 236 (1956) 397–410.
[11] S. Pan, C. Zhao, P. Wei, F. Ren, Sliding wear of CoCrNi medium-entropy alloy at elevated temperatures: wear mechanism transition and subsurface microstructure evolution, Wear. 440 (203108) (2019) 1–13.
[12] F.E. Kennedy, Y. Lu, I. Baker, Contact temperatures and their influence on wear during pin-on-disk tribotesting, Tribol. Int. 56 (2013) 534–542.
[13] F. Stott, The role of oxidation in the wear of alloys, Tribol. Int. 31 (1998) 61–71.
[14] H. So, The mechanism of oxidational wear, Wear 184 (1995) 161–167.
[15] B.J. Johnson, F.E. Kennedy, I. Baker, Dry sliding wear of NiAl, Wear 192 (1996) 241–247.
[16] NIST X-ray Photoelectron Spectroscopy Database, NIST Standard Reference Database Number 20, 20899 National Institute of Standards and Technology, Gaithersburg MD, 2000, https://doi.org/10.18434/T4T88K (retrieved [date of access]).
[17] Metals Handbook, Volume 1: Properties and Selection of Irons, Steels and High-Performance Alloys, ASM International, Materials Park, OH, 1990.
[18] K. Jin, S. Mu, K. An, W.D. Porter, G.D. Samolyuk, G.M. Stocks, H. Bei, Thermophysical properties of Ni-containing single-phase concentrated solid solution alloys, Mater. Des. 117 (2017) 185–192.
[19] C.Y. Ho, T.K. Chu, Electrical resistivity and thermal conductivity of nine selected AISI stainless steels, Thermophysical and electronic properties information analysis center lafayette in. no. CINDAS-45, 1977, p. 21.
[20] D.A. Rigney, Comments on the sliding wear of metals, Tribology Int 30 (1997) 361–367.